STUDIA UBB CHEMIA, LVII, 3, 2012 (p. 259 – 266)
(RECOMMENDED CITATION)

HARD CHEMICAL CONSTITUENT EVIDENCE IN FERROMANGANESE ALLOYED POWDER FeMn80C20

CRISTIAN SUCIU[1], GEORGE ARGHIR[1], PAUL BERE[2]

ABSTRACT. The mechanical properties of sintered steels are depending mainly on the powder microstructure. The paper presents studies of ferromanganese powder obtained by milling. The X-ray diffraction analysis evidenced two chemical compounds: the major compound is $FeMn_4$, and some traces of complex ferromanganese carbide $Fe_{1.1}Mn_{3.9}C_2$. The carbide hardness is 2365 $HV_{0.02}$. They are dispersed in the major micro structural constituent, α Mn phase. The observed microstructure prove that α Fe appears only as phase in a pearlite like eutectoid constituent. It appears as a grey lamellar micro structural constituent having an average grain size of 50 μm. This constituent feature present hardness values lower than 715 $HV_{0.02}$. Finally, we could conclude that the particle size do not affects the powder composition and micro structural constituents' distribution. The particle size affects only the technological properties as apparent density and the flow rate.

Keywords: *ferromanganese powder, hard compounds, phase distribution*

INTRODUCTION

The hard chemical and intermetallic compounds are intensively investigated in order to achieve a better wear resistance designed for a wide range of industrial and technical applications [1, 2]. Several methods for the surface hardening were found in the literature. Considering iron or low alloyed steel as the bulk base, the wear surface of the part needs an improved hardness. One of the current method used for surface hardness improvement is the coating with hard iron compounds with some different atomic species such Al, Ti, and some of the newest iron carbon fullerites [3 - 5]. The above mentioned studies reveal that a special microstructure occur during surface enrichment with Al. Ti based hard compounds formation are relative to surface nitrating or nitro - carburizing processes [6, 7]. Thus, it means that the alloying micro-structural components involved in the hardening layers play the most important role in the wear strength improvement success. The

[1] *Technical University of Cluj - Napoca, Faculty of Materials Science and Environmental Engineering, Muncii Ave., No. 103-105, RO-400641 Cluj-Napoca, Romania, suciucristianteo@yahoo.com*
[2] *Technical University of Cluj-Napoca, Faculty of Machine Building, Muncii Ave., No. 103-105, RO-400641 Cluj-Napoca, Romania*

hard compound development at micro-structural is very important but not enough for a proper wear strength improvement; this requires also a very good dispersion of the hard component grains among the bulk part microstructure. A well-controlled powder mixture allows a good wear resistance improvement via plasma spray coating as well as via powder metallurgy processes [8 - 10].

The most important hardening element in alloys is manganese due to its hard microstructure developed when is alloyed with iron. As it is known, manganese alloys are very suitable for automobile industry and military applications [11, 12]. Nowadays is a more pronounced tendency to replace expensive alloying elements with less expensive ones. Recent studies points out the manganese compounds importance in the powder metallurgy field [13, 14]. There were reported refined structures obtained by alloying during the sintering process as a consequence of atom species diffusion [13].

Considering the previously mentioned aspects as a pertinent hypothesis it results that the hardening effect in iron manganese alloys are strongly related with the micro-structural aspect of hard compound grains as well as their distribution. In such cases, the initial pre alloyed manganese powder is essential. Finally the aim of this research is to investigate the manganese hard compound distribution in the micro-structure of the FeMn80C20 pre alloyed powder.

RESULTS AND DISCUSSION

The initial FeMn80C20 powder was sieved according to the particle size class; the results are presented in Table 1. The predominant particle size class is situated between 125 ÷ 250 μm having almost 40 wt. % of the total powder amount. We would further refer to this value as average particle size.

Table 1. Powder particles size (wt. %)

Particle size (μm)	< 63	63 ÷ 71	71 ÷ 80	80 ÷ 100	100 ÷ 125	125 ÷ 250	250 ÷ 315	> 315
FeMn80C20,%	9.43	1.66	1.29	4.06	7.21	37.71	24.22	14.42

There are some particles with bigger size (around 38 %) distributed widely between 250 ÷ 315 μm. The refined particles are less represented in powder distribution; despite this we notice a significant amount of 9.43 wt % under 63 μm. These finest particles could be important enough in a further surface hardening due to their ability to be assimilate by the host microstructure.

The powder apparent density and the flow rate are presented in Table 2.

Table 2. Apparent density and flow rate of powder

Sample	Apparent density, (g/cm^3)	Flow rate, (sec/50 g)
FeMn80C20	3.38	37

Both technological parameters are affected by the micro structural particles distribution. The obtained values are in agreement with the observed distribution. The smaller particles fill up the spaces between the greater particles reducing empty spaces fact which increases the apparent density to a value closer to the bulk density. Still, we notice a significant difference due to the presence of the bigger particles. The flow rate is also affected by the particle size. The non-uniform particle distribution as presented in Table 1 conducts to a relatively good flow rate of the ferro manganese powder.

The chemical composition of the utilized powder is another important parameter which must to be followed. We performed a mass spectrometry determination for the initial powder in order to check the main elements. The results are in good agreement with the composition provided by the powder manufacturer is presented in the Table 3.

Table 3. Chemical composition of powder

Sample	C, (%)	Si, (%)	Fe, (%)	P, (%)	Mn, (%)
FeMn80C20	2.32	3.03	16.00	0.17	78.36

The ensemble view of the FeMn80C20 powder microstructure after polishing and nital chemical etching is presented in Figure 1a. Particles having polyhedral borders were identified. This fact proves the brittle nature of the powder which is close related to the high hardness. As mentioned in the experimental section the powder was produced by grinding, fact observed by the particle shape.

The chemical etching reveals the microstructure of the particle insight: larger white areas having around of 175 μm are surrounded by finest black grains which could be some intermediary compounds. Several darken areas are also observed close to the particles borders.

The microstructure observed at average magnification, Figure 1b, reveals more clearly the micro–constituents. There are observed few greater white grains surrounded with some lamellar areas having around of 50 μm average diameter. The structures of lamellar grains are pearlite like, which corresponds to the mentioned eutectoids in the Fe-Mn equilibrium diagram. There are also observed finest grains having over 20 μm diameter dark colored which could belongs to some complexes of FeMn or FeMnC compounds.

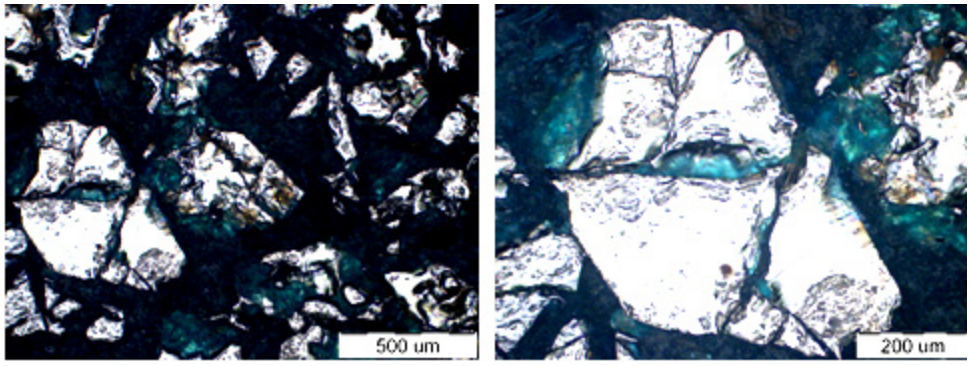

a) b)

Figure 1. The microstructure of FeMn80C20 powder:
a) low magnification and; b) average magnification. Nital 3%

Considering the equilibrium conditions for the FeMn binary system at the powder composition we have a mixed microstructure formed by α Mn grains very similar to ferrite in steels, and eutectoid grains formed by a fine mixture of α Mn and α Fe. The micro hardness results, Table 4, agrees the microstructural observations, α Mn (bright white grains) being harder than eutectoid grains.

Table 4. Micro hardness of the FeMn80C20 powder constituents

Grain type, colour	Average grain diameter, (μm)	Microhardness ($HV_{0.02}$)
Gray shade (lamellar compound)	50	715
Bright white (ferrite like)	175	1695
Dark	20	2365

The darken grains feature a higher hardness over the other microstructural compounds corresponding to the equilibrium diagram. Perhaps during alloying process and further cooling there were developed some chemical compounds corresponding to a non-equilibrium state. Such compounds appear often in alloyed steels at different thermal gradients [15].

The micro-structural characteristics must to be confronted with the crystalline phase analysis. The proper phase identification in the ferromanganese powder could be performed in optimum conditions only with the X-ray diffraction technique [16, 17]. Each particle class sample was subjected to the X-ray diffraction investigation. The resulted patterns are presented in Figure 2. All samples feature a pronounced crystalline aspect which is in concordance

with the micro-structural observations presented in Figure1. The diffractions peaks are well developed in full agreement with the polycrystalline aspect of metals and alloys. We observed, in Figure 2a, a significant influence of particle size class on the diffraction peaks shape. The greater particles conduct to a relative smooth baseline and vigorous peaks, case of Figure 2 a-c. This is due to their relative large surface which allows a good focalization of the incident X-ray. The average particles/grains, feature well developed XRD pattern along with a slightly tendency of "noise" at the baseline level, case of Figure 2 d-f. The smaller particles induce a significant "noise" at the pattern baseline due to their small size associated with a random orientation. Thus, the relevant peaks are more enhanced mainly because the finest and randomly oriented particles in the sample surface, case observed for Figure 2 g and h.

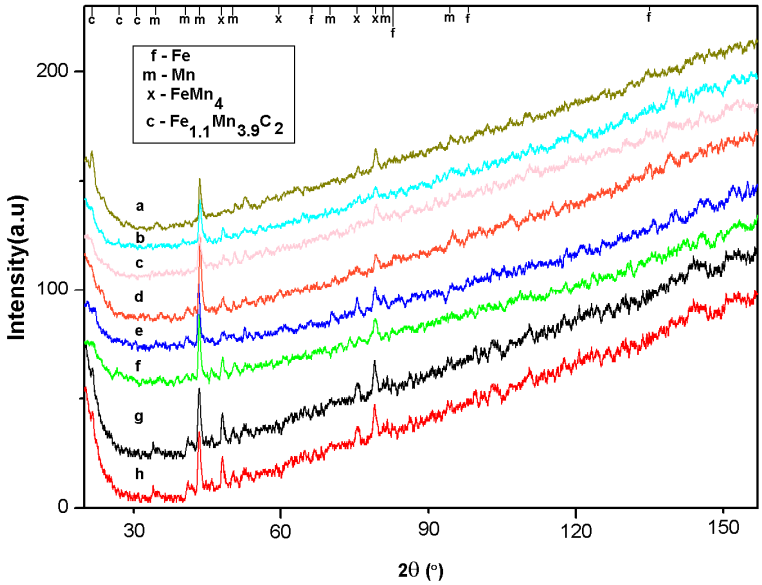

Figure 2. X-ray diffraction pattern for FeMn80C20 powder at different grain size: a) > 315 μm, b) 250 ÷ 315 μm, c) 125 ÷ 250 μm, d) 100 ÷ 125 μm, e) 80 ÷ 100 μm, f) 71 ÷ 80 μm, g) 63 ÷ 71 μm, and h) 0 ÷ 63 μm.

The XRD investigation of ferromanganese powder according to their particle size classes allows a full characterization of the considered material. We notice that relevant peaks appears in all obtained XRD patterns, relevant peaks appear in all obtained XRD patterns, Figure 2 only small variation of their relative intensity was observed. The diffraction angles do not varies with the particles size. All aspects reveal that the investigated ferromanganese powder is homogeneous from the point of view of phase composition.

The main phase component of the ferromanganese sample is the α Mn. Considering the relative intensities and the structure factor we could estimate that the amount of α Mn phase is around of 75 wt. %, which result in good agreement with the mass spectrometry results.

Other identified phase is the ferromanganese compound $FeMn_4$ which is well represented by four diffraction peaks with relative intensities ranging from 10% to 50%. This proves to be related to darken, hard compound revealed by microscopic investigation. This type of compound is mentioned in literature as results of the quenching process [18]. Its presence in the composition of the investigated ferromanganese powder could be explained only by some faster thermal gradients involved during the powder manufacturing. However, α Fe as single phase was identified only with weaker peaks under 25% relative intensity. This fact may confirm that a significant iron amount was consumed by the formation of $FeMn_4$ hard compound. The α Fe phase appears, in the investigated powder sample, only as component in the lamellar grey compound (eutectoid like).

Finally, the carbon was evidenced in the phase structure of the ferromanganese powder as $Fe_{1.1}Mn_{3.9}C_2$ carbide. This phase prove to be as trace levels the corresponding diffraction peaks being relatively weak. However, such carbide is also a hard compound which could locally increase the sample micro hardness.

The micro hardness tests confirm the connections between identified phases and the microstructure. The greater micro hardness result appears for the dark smallest spots in the microstructure (as report in Table 4). The weaker hardness appears on the pearlite like compound where free α Fe could be found.

CONCLUSIONS

The ferromanganese powder is very important for various applications where surface hardening is required mainly for the intensive wear surfaces. We investigate a commercial type of ferromanganese powder with 80% Mn in order to establish the hard chemical components or constituents.

The X-ray diffraction analysis evidenced two chemical compounds able to increase the sample hardness: the major compound is $FeMn_4$, it is followed by some traces of complex ferromanganese carbide $Fe_{1.1}Mn_{3.9}C_2$. This compounds are fine distributed in the α Mn phase, fact in good concordance with the microscopy investigation. The very hard dark spots have the grain size below 20 μm. Their micro hardness is 2365 $HV_{0.02}$.

Free α Fe phase was evidenced by the X-ray diffraction. The observed microstructure prove that α Fe appears only as phase in a pearlite like eutectoid constituent. It appears as a grey lamellar micro structural constituent having an average grain size of 50 μm. This constituent feature a hardness of 715 $HV_{0.02}$.

Finally, we could conclude that the particle size do not affects the powder composition and micro structural constituents' distribution. The particle size affects only the technological properties as apparent density and the flow rate.

EXPERIMENTAL SECTION

The ferromanganese powder FeMn80C20 was produced by Elkem Ferromanganese Sauda, Norway, according to the E.U. prescriptions. The samples were prepared according to their particle size class by sieving a roughly un-uniform FeMn80C20 ferromanganese powder. The powder sieving and distribution on the particle classes was performed according to the prescription European Union standards SR EN 2449. The apparent density was measured and calculated according to the prescriptions SR EN 23923, meanwhile the powder flow rate was determined according to ISO 4490, using a flow meter with a diameter of 2.54 mm.

The powder chemical composition was determined on an inductive coupled plasma mass spectrometer type Elan DRC (ICP-MS). For instance, the powder sample (e.g. 1 gram) was melted in a specific crucible as demanded by the spectrometer requirements.

The powder was integrated in resin samples for the microstructure analysis. The samples were polished and etched with 3% Nital, for metallographic investigations. The microstructural analysis and photography was done on an Olympus GX51 microscope. The micro-hardness $HV_{0.02}$ was measured on a Carl Zeiss Neophot 2 microscope with a micro-hardness tester.

The X-ray diffraction analysis was performed on a Dron 3 diffract meter equipped with data acquisition module. A monochrome Cu K_α radiation was used. The crystalline compounds were identified from the X-ray diffraction pattern using Match 1.0 Standard Database powered by Crystal Impact Company.

ACKNOWLEDGMENTS

This paper was supported by the project "Doctoral studies in engineering sciences for developing the knowledge based society-SIDOC" contract no. POSDRU/88/1.5/S/60078, project co-funded from European Social Fund through Sectorial Operational Program Human Resources 2007-2013 and by the project "Develop and support multidisciplinary postdoctoral programs in primordial technical areas of national strategy of the research - development - innovation" 4D-POSTDOC, contract nr. POSDRU/89/1.5/S/52603.

REFERENCES

1. Ni. Wangyang, Y.T. Cheng, D.S. Grummon, *Surface and Coatings Technology*, **2006**, *201*, 1053.
2. J.D. Bressan, R. Hesse, E.M. Silva, *Wear*, **2001**, *250*, 561.
3. D.E. Alman, J.A. Hawk, J.H. Tylczak, C.P. Dogan, R.D. Wilson, *Wear*, **2001**, *251*, 875.
4. S. PalDey, S.C. Deevi, *Materials Science and Engineering*, **2003**, *A342*, 58.
5. O.P. Tchernogorova, O.A. Bannykh, V.M. Blinov, E.I. Drozdova, A.A. Dityatev , N.N. Melnik, *Materials Science and Engineering*, **2001**, *A299*, 136.
6. L.L Pranevicius, P. Valatkevicius, V. Valincius, C. Templier, J.-P. Riviere, L. Pranevicius, *Surface and Coatings Technology*, **2002**, *156*, 219.
7. Ph. Roquiny, G. Mathot, G. Terwagne, F. Bodart, P. van den Brande, *Nuclear Instruments and Methods in Physics Research B*, **2000**, *161-163*, 600.
8. H. Eschnauer, E. Lugscheider, *Thin Solid Films*, **1984**, *118*, 421.
9. H. Bhat, H. Herman, *Thin Solid Films*, **1982**, *95*, 227.
10. A. Salak, M. Selecka, *Materials Science Forum*, **2011**, *672*, 55.
11. Y.N. Dastur, W. C. Leslie, *Metalurgical Transactions*, **1981**, *12A*, 749.
12. J. Tianfu, Z. Fucheng, *Materials Letters*, **1997**, *31*, 275.
13. M. Selecka, A. Salak, D. Jukubeczyova, *Materials Science Forum*, **2011**, *672*, 59.
14. A. Salak, M. Selecka, *Powder Metallurgy*, **2008**, *51*, 327.
15. P. Nurthen, O. Bergman, I. Hauer, *PM 2008 Word Congress*, Washinton, USA, **2008**.
16. G. Arghir, "Caracterizarea metalelor şi aliajelor prin difractie cu raze X", Litografia Universitaţi Tehnice din Cluj Napoca, **1993**.
17. A. Clearfield, H. Reibenspies, N. Bhuvanesh, "Principles and Applications of Powder Diffraction", Blackwell Publishing Ltd., **2008**.
18. A. Westgreen, G. Phragmen, *Z. Physics*, **1925**, *33*, 784.